Electromagnetically induced absorption due to transfer of population in degenerate two-level systems

C. Goren,[1] A. D. Wilson-Gordon,[2] M. Rosenbluh,[1] and H. Friedmann[2]
[1]*Department of Physics, Bar-Ilan University, Ramat Gan 52900, Israel*
[2]*Department of Chemistry, Bar-Ilan University, Ramat Gan 52900, Israel*
(Received 19 May 2004; published 21 October 2004)

We predict the occurrence of electromagnetically induced absorption (EIA) in cycling degenerate two-level transitions where $F_e=F_g+1$ and $F_g>0$, interacting with pump and probe lasers with the same polarization. The EIA is due to transfer of population (TOP) between the Zeeman levels of the ground hyperfine state, rather than transfer of coherence (TOC) which occurs for perpendicularly polarized lasers. We model EIA-TOP using a double two-level system (TLS) which we compare with the four-level *N* system, which models EIA-TOC. When the pump intensity is low, both models give an EIA peak at line center. The effect of introducing phase-changing collisions is studied, in the presence and absence of Doppler broadening, for both the double TLS and *N* systems. In the presence of phase-changing collisions, the central EIA peaks are narrowed in both models and persist to higher pump Rabi frequencies than in the absence of collisions. In the double TLS, in the presence of Doppler broadening, the central EIA-TOP peak becomes narrower and does not develop a dip in its center, in contrast to the *N* system. The central dip that appears in the Doppler-broadened EIA-TOC spectrum can be wiped out by adding phase-changing collisions. We demonstrate that EIA-TOP can be obtained for realistic atomic transitions interacting with lasers that have the same polarization.

DOI: 10.1103/PhysRevA.70.043814 PACS number(s): 42.50.Gy, 42.50.Nn, 42.65.−k

I. INTRODUCTION

Electromagnetically induced absorption (EIA) has been studied extensively, both experimentally and theoretically. In the original experiments, EIA was obtained for perpendicularly polarized pump and probe lasers, interacting with a cycling degenerate two-level transition in which $F_e=F_g+1$ and $F_g>0$ [1,2]. For this case, EIA was shown to be due to transfer of coherence (TOC), via spontaneous emission, from the excited to the ground states [3–5]. In later experiments, EIA was also found for noncycling degenerate two-level systems (TLS's) [6,7] and in systems where $F_g \geqslant F_e>0$ [7].

A different type of EIA, due to transfer of population (TOP), was predicted by us [5] for a cycling, degenerate TLS where $F_e=F_g+1$ and $F_g>0$, interacting with lasers of the same polarization. This EIA-TOP can occur provided the decay out of the degenerate TLS from the ground state is greater than from the excited state [8]. This condition is fulfilled if the ground-state population is transferred by collisions to a nearby state that does not interact with the lasers, and cannot be populated by spontaneous emission from the excited state [5]. EIA has also been predicted for a three-level Λ system interacting with a standing wave [9], and for a nearly degenerate tripod system interacting with a σ polarized pump and a π polarized probe [10]. In this paper, we show that EIA-TOP can be obtained even in the absence of inelastic collisions, provided the intensity of the pump laser that interacts with the degenerate two-level system is sufficiently low. In order to model this version of EIA-TOP, we consider a double TLS, pumped and probed by lasers of the same polarization [see Fig. 1(a)]. The double TLS interacts with a pump laser of frequency ω_1, which couples level g_1 to e_1, and level g_2 to e_2, with Rabi frequencies, V_1 and V_2. The e_2 to g_1 transition is forbidden by selection rules. The probe laser of frequency ω_p also couples levels g_1 to e_1, and g_2 to e_2, with Rabi frequencies V_{p_1} and V_{p_2}. This model corresponds to a cycling degenerate TLS, where $F_e>F_g>0$, interacting with σ_+ polarized pump and probe lasers.

We compare the probe absorption spectra for the double TLS which is a model for EIA-TOP, with those of the *N* system [11] [see Fig. 1(b)] which is a model for EIA-TOC [3,4]. We find that both model systems give an EIA peak at line center, when the pump intensity is low. However, the probe absorption spectra are completely different at higher pump intensity: the spectrum of the double TLS is similar to that of a simple TLS, while the spectrum of the *N* system has

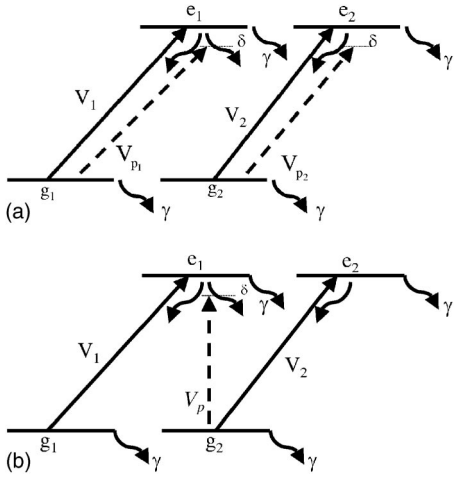

FIG. 1. (a) Energy-level scheme for the double TLS system interacting with two resonant pumps, V_1 and V_2, and two tunable probes, V_{p1} and V_{p1}. (b) Energy-level scheme for the four-level *N* configuration atom interacting with two resonant pumps, V_1 and V_2 and a tunable probe, V_p.

four peaks [11]. We also study the effect of introducing phase-changing collisions [12,13] in both models, and find that the EIA peaks that appear at low pump intensity become narrower in both cases, and persist to higher pump intensities than in the absence of such collisions. At these intensities, which are different for each of the models, the EIA peak is surrounded by a broader dip.

When the double TLS is Doppler broadened in the absence of phase-changing collisions, the spectrum is characterized by EIA at low pump intensities. On increasing the intensity, the spectrum resembles that of a simple TLS, namely a dead zone [14,15], but with the addition of a small EIA peak at line center which does not exist in the absence of Doppler broadening. When phase-changing collisions are included, the spectra for both models resemble those obtained in the absence of Doppler broadening, namely, a central EIA peak surrounded by a wider dip. In both models, Doppler broadening increases the width of the dip which still remains sub-Doppler. However, the central EIA peak behaves differently in each case: in the double TLS case, the peak becomes narrower on Doppler broadening but, in contrast to the *N* system [11], does not develop a dip at line center. In addition, we show here that the dip that appears at line center in the probe absorption spectrum of the *N* system, in the presence of Doppler broadening, can be wiped out by introducing phase-changing collisions.

We calculate the EIA-TOP for realistic atomic transitions and show that both σ_+ and linearly polarized lasers give EIA-TOP without inelastic collisions.

II. EQUATIONS OF MOTION

We begin by writing the equations of motions for the double TLS of Fig. 1(a):

$$\dot{\rho}_{g_1g_1} = -\gamma(\rho_{g_1g_1} - \rho^{eq}_{g_1g_1}) + \gamma_{e_1g_1}\rho_{e_1e_1} - i(V_1^*\rho_{e_1g_1} - V_1\rho_{g_1e_1}), \tag{1}$$

$$\dot{\rho}_{g_2g_2} = -\gamma(\rho_{g_2g_2} - \rho^{eq}_{g_2g_2}) + \gamma_{e_1g_2}\rho_{e_1e_1} + \Gamma\rho_{e_2e_2} - i(V_2^*\rho_{e_2g_2} - V_2\rho_{g_2e_2}), \tag{2}$$

$$\dot{\rho}_{e_ig_i} = -(i\omega_{e_ig_i} + \Gamma_{e_ig_i})\rho_{e_ig_i} - iV_i(\rho_{g_ig_i} - \rho_{e_ie_i}), \tag{3}$$

$$\dot{\rho}_{e_ie_i} = -(\gamma + \Gamma)\rho_{e_ie_i} - i[V_i\rho_{g_ie_i} - V_i^*\rho_{e_ig_i}], \tag{4}$$

where $i=(1,2)$. In Eqs. (1)–(4), γ is the decay rate due to the time of flight of the atoms through the laser beam, Γ is the decay rate of the excited states due to spontaneous emission, $\gamma_{e_1g_1}$ and $\gamma_{e_1g_2}$ are the decay rates from e_1 to g_1 and g_2, which are determined by the branching ratio of the atomic transition, so that $\gamma_{e_1g_1}=A^2\Gamma$ and $\gamma_{e_1g_2}=B^2\Gamma$, where $A^2+B^2=1$. $\Gamma_{e_ig_i}=\frac{1}{2}\Gamma+\Gamma^*$ is the transverse decay rate for the transition between states e_i and g_i, where Γ^* is the rate of phase changing collisions. Here, we have neglected population transferring collisions between the two ground states. This is generally valid for experiments in alkali vapors or beams [16,17], unless we specifically choose the experimental parameters so that they become significant as in Ref. [5]. In writing the equations of motion we have used the rotating-wave approximation in which

$$V_i = V_i(\omega_1)\exp(-i\omega_1 t) + \text{c.c.}, \tag{5}$$

$$V_{i_p} = V_{i_p}(\omega_p)\exp(-i\omega_p t) + \text{c.c.} \tag{6}$$

In order to calculate the probe absorption and refraction to first order in the probe, and to all orders in the pump, we solve Eqs. (1)–(4) in two stages. In the first stage, the system interacts only with the pump so that the off-diagonal density matrix elements $\rho_{e_1g_1}$ and $\rho_{e_2g_2}$ can be expressed in terms of their Fourier amplitudes as

$$\rho_{e_ig_i} = \rho_{e_ig_i}(\omega_1)\exp(-i\omega_1 t), \tag{7}$$

where $i=(1,2)$. Inserting Eqs. (5) and (7) into Eqs. (1)–(4), we obtain the following set of linear equations for the Fourier amplitudes:

$$\dot{\rho}^0_{g_1g_1} = -\gamma(\rho^0_{g_1g_1} - \rho^{eq}_{g_1g_1}) + \gamma_{e_1g_1}\rho^0_{e_1e_1} + i[V_1(-\omega_1)\rho_{e_1g_1}(\omega_1) - V_1(\omega_1)\rho_{g_1e_1}(-\omega_1)], \tag{8}$$

$$\dot{\rho}^0_{g_2g_2} = -\gamma(\rho^0_{g_2g_2} - \rho^{eq}_{g_2g_2}) + \gamma_{e_1g_2}\rho^0_{e_1e_1} + \Gamma\rho^0_{e_2e_2} + i[V_2(-\omega_1)\rho_{e_2g_2}(\omega_1) - V_2(\omega_1)\rho_{g_2e_2}(-\omega_1)], \tag{9}$$

$$\dot{\rho}_{e_ig_i}(\omega_1) = -[i(\omega_{e_ig_i} - \omega_1) + \Gamma_{e_ig_i}]\rho_{e_ig_i}(\omega_1) + iV_i(\omega_1)(\rho^0_{g_ig_i} - \rho^0_{e_ie_i}), \tag{10}$$

$$\dot{\rho}^0_{e_ie_i} = -(\gamma + \Gamma)\rho^0_{e_ie_i} + i[V_i(\omega_1)\rho_{g_ie_i}(-\omega_1) - V_i(-\omega_1)\rho_{e_ig_i}(\omega_1)]. \tag{11}$$

Equations (8)–(11) are solved in the steady state by setting the time derivatives to zero.

In the second stage, the probe field is included to first order, so that the density matrix elements $\rho_{e_ig_i}$ now oscillate at three frequencies [18–20]: the pump frequency ω_1, the probe frequency ω_p, and the four-wave mixing frequency $2\omega_1-\omega_p$ so that

$$\rho_{e_ig_i} = \rho_{e_ig_i}(\omega_1)\exp(-i\omega_1 t) + \rho_{e_ig_i}(\omega_p)\exp(-i\omega_p t) + \rho_{e_ig_i}(2\omega_1-\omega_p)\exp[-i(2\omega_1-\omega_p)t]. \tag{12}$$

Similarly, the populations can be written in terms of their Fourier amplitudes as

$$\rho_{g_ig_i} = \rho^0_{g_ig_i} + \rho_{g_ig_i}(\omega_p-\omega_1)\exp[-i(\omega_p-\omega_1)t] + \rho_{g_ig_i}(\omega_1-\omega_p)\exp[-i(\omega_1-\omega_p)t]. \tag{13}$$

Inserting Eqs. (5), (6), (12), and (13) in Eqs. (1)–(4), we obtain the following set of linear equations for the Fourier amplitudes:

$$\dot{\rho}_{g_1g_1}(\omega_1-\omega_p) = -[i(\omega_p-\omega_1)+\gamma]\rho_{g_1g_1}(\omega_1-\omega_p) + \gamma_{e_1g_1}\rho_{e_1e_1}(\omega_1-\omega_p) + i[V_1(-\omega_1) \times \rho_{e_1g_1}(2\omega_1-\omega_p) - V_1(\omega_1)\rho_{g_1e_1}(-\omega_p) + V_{p_1}(-\omega_p)\rho_{e_1g_1}(\omega_1)], \quad (14)$$

$$\dot{\rho}_{g_2g_2}(\omega_1-\omega_p) = -[i(\omega_p-\omega_1)+\gamma]\rho_{g_2g_2}(\omega_1-\omega_p) + \gamma_{e_1g_2}\rho_{e_1e_1}(\omega_1-\omega_p) + \Gamma\rho_{e_2e_2}(\omega_1-\omega_p) + i[V_2(-\omega_1)\rho_{e_2g_2}(2\omega_1-\omega_p) - V_2(\omega_1) \times \rho_{g_2e_2}(-\omega_p) + V_{p_2}(-\omega_p)\rho_{e_2g_2}(\omega_1)], \quad (15)$$

$$\dot{\rho}_{e_ig_i}(\omega_p) = -[i(\omega_{e_ig_i}-\omega_p)+\Gamma_{e_ig_i}]\rho_{e_ig_i}(\omega_p) + i\{V_i(\omega_1)[\rho_{g_ig_i}(\omega_p-\omega_1)-\rho_{e_ie_i}(\omega_p-\omega_1)] + V_{p_i}(\omega_p)(\rho^0_{g_ig_i}-\rho^0_{e_ie_i})\}, \quad (16)$$

$$\dot{\rho}_{e_ig_i}(2\omega_1-\omega_p) = -\{i[\omega_{e_ig_i}-(2\omega_1-\omega_p)]+\Gamma_{e_ig_i}\} \times \rho_{e_ig_i}(2\omega_1-\omega_p) + i\{V_i(\omega_1) \times [\rho_{g_ig_i}(\omega_1-\omega_p)-\rho_{e_ie_i}(\omega_1-\omega_p)]\}, \quad (17)$$

$$\dot{\rho}_{e_ie_i}(\omega_1-\omega_p) = -[i(\omega_p-\omega_1)+\gamma+\Gamma]\rho_{e_ie_i}(\omega_1-\omega_p) + i[V_i(\omega_1)\rho_{g_ie_i}(-\omega_p) - V_i(-\omega_1) \times \rho_{e_ig_i}(2\omega_1-\omega_p) - V_{p_i}(-\omega_p)\rho_{e_ig_i}(\omega_1)]. \quad (18)$$

The equations for $\rho_{a_ia_i}(\omega_p-\omega_1)$ for $a=(g,e)$ and $i=(1,2)$ can easily be written by analogy with Eqs. (14), (15), and (18).

III. PROBE ABSORPTION IN DOUBLE TLS

The probe absorption for the double TLS shown in Fig. 1(a) is given by [5]

$$\alpha \propto \mathrm{Im}[A^2\rho_{e_1g_1}(\omega_p)/V_{p_1} + \rho_{e_2g_2}(\omega_p)/V_{p_2}], \quad (19)$$

which is derived assuming that $\mu_{e_1g_1}=A\mu_{e_2g_2}$ so that $V_1=AV_2$ and $V_{p_1}=AV_{p_2}$. In our calculations we take $A=0.816$ which is the value that corresponds to the $F_g=2\rightarrow F_e=3$ cycling transition in ^{87}Rb.

As can be seen from Eq. (19) and Fig. 1(a), the total probe absorption for the double TLS results from interference between the two transitions that interact with the probe. The transitions are not equivalent. This is due to the fact that e_1 decays into both the ground states, g_1 and g_2, whereas e_2 decays into only the g_2 ground state. Let us compare each of the interacting TLS's with the single TLS discussed in Ref. [8]. For this purpose, we assume that there are no population transferring collisions between the two TLS's. In the first transition with probe Rabi frequency V_{p1}, the total decay rate of the excited state out of the system is $\gamma_{e_1}=\gamma+\gamma_{e_1g_2}$ which is greater than the decay rate of the ground state, γ. As discussed in Ref. [8] this leads to a narrow dip at line center in the probe absorption spectrum [see Fig. 2(a)]. In the second transition where the probe Rabi frequency is V_{p_2}, the decay rate out of the system from the excited state is equal to that of the ground state $\gamma_{e_2}=\gamma_{g_2}=\gamma$. However, TOP from the first TLS compensates for the depletion of the ground-state population by the pump, thereby increasing the absorption. This leads [8] to a narrow peak at line center [see Fig. 2(b)]. When the contributions of the separate TLS's are added, a peak is obtained in the probe absorption spectrum, as shown in Fig. 2(c). When population transferring collisions between the ground states are included, the narrow features are wiped out, as was shown in our previous paper [5] where EIA-TOP resulted from population transfer to and from states that did not interact with the lasers.

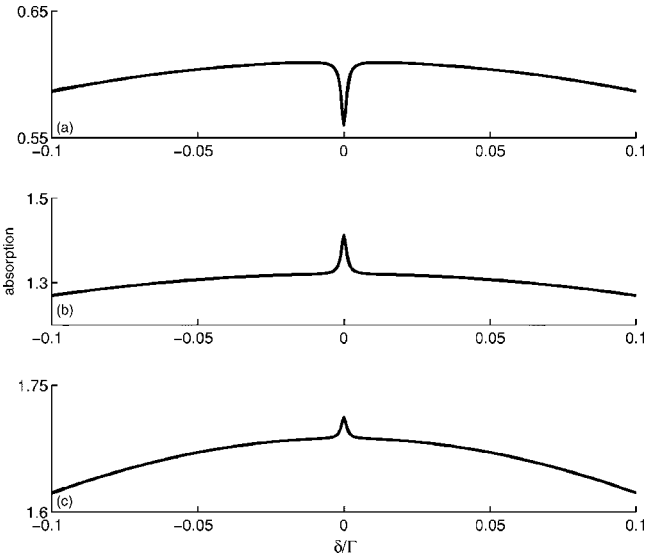

FIG. 2. Probe absorption spectrum for the double TLS system: (a) contribution from first transition, $\mathrm{Im}(A^2\rho_{e_1g_1})\Gamma/V_{p_1}$, (b) contribution from second transition, $\mathrm{Im}(\rho_{e_2g_2})\Gamma/V_{p_2}$, and (c) total probe absorption spectrum: $\mathrm{Im}[(A^2\rho_{e_1g_1})/V_{p_1}+(\rho_{e_2g_2})/V_{p_2}]\Gamma$, for $V_2/\Gamma=0.1$, $V_1=0.816V_2$ and $\gamma/\Gamma=0.001$.

In the next section, we compare the probe absorption spectra for the double TLS with those of the N system [11]. We will see that the narrow features disappear with increasing pump intensity as in the ordinary TLS [8].

IV. COMPARISON OF THE DOUBLE TLS AND THE N SYSTEM

The probe absorption for the double TLS is compared with that of the N system [11] for the case of a weak probe in Fig. 3. The left column refers to the double TLS and the right column refers to the N system. We see that at low pump intensities, the probe absorption in both cases is characterized by an EIA peak [Figs. 3(a) and 3(b)]. When the pump intensity increases, the width of both EIA peaks increases [Figs. 3(c) and 3(d)], with significant enhancement of the narrow peak in the case of the N system [Fig. 3(d)]. As the intensity is increased further, the EIA peaks disappear, as discussed in Refs. [8,11]. At even higher pump intensities,

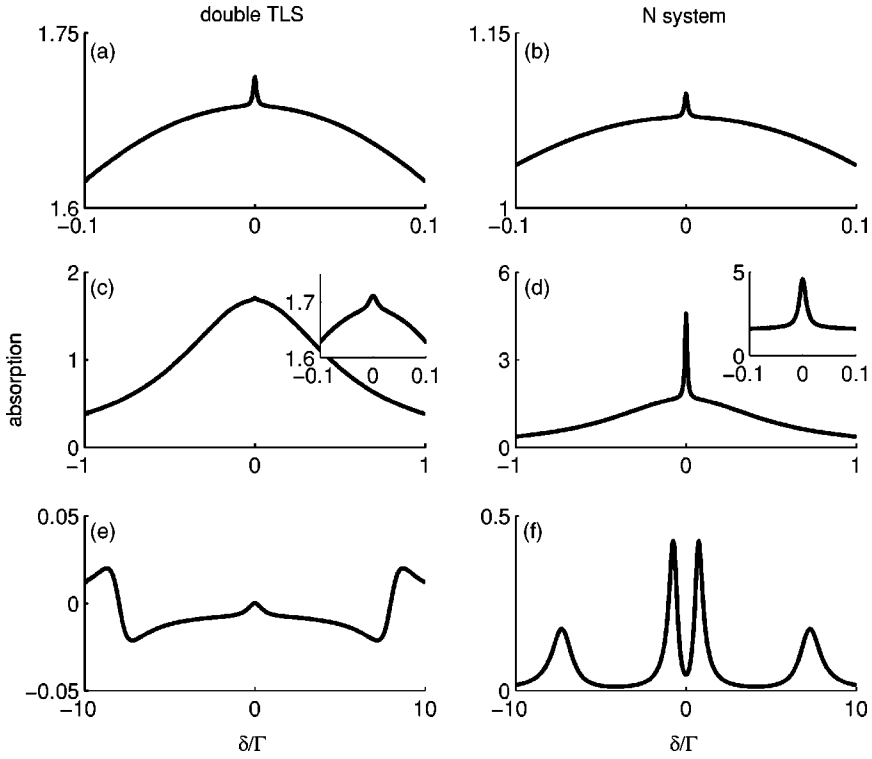

FIG. 3. Calculated probe absorption spectra for the double TLS (left column) and for the N system (right column). In (a) and (b), $V_2/\Gamma=0.01$, in (c) and (d), $V_2/\Gamma=0.1$, and in (e) and (f), $V_2/\Gamma=4$. In all the graphs $V_1=0.816V_2$ and $\gamma/\Gamma=0.001$.

the population is swept into levels e_2 and g_2. Consequently the absorption spectrum of the double TLS reduces to that of a single TLS [Fig. 3(e)], whereas the absorption spectrum of the N system acquires four peaks centered at frequencies $\pm(V_1\pm V_2)$ [Fig. 3(f)]. The origin of the four peaks can be explained in terms of the dressed states produced by the two pumped transitions which have different Rabi frequencies [11].

V. EFFECT OF A BUFFER GAS ON THE EIA SPECTRA

The effect of phase-changing collisions induced by a buffer gas have recently been discussed for a Λ system [12,13]. Here we compare the effect of the phase-changing collisions on both types of EIA spectra.

A. Double TLS

In Fig. 4, we compare the absorption spectra for the double TLS, in the absence and presence of phase-changing collisions. At low intensities, the collisions broaden the background absorption, leaving the central feature almost unaffected [see Figs. 4(a) and 4(b)]. As the pump intensity increases [Figs. 4(c) and 4(d)], the population is swept into the second TLS, and the spectra with and without phase changing collisions resemble those of a single TLS [21], except for a residual EIA peak at line center in the presence of the phase-changing collisions [Fig. 4(d)]. This structure, consisting of a dip of width of the order of Γ and a narrow central peak, can be predicted from the analytical expressions given in Ref. [18]. On further increase in the pump intensity [Figs. 4(e) and 4(f)], the residual EIA peak disappears. The occurrence of the residual peak can be understood by noting that the introduction of phase-changing collisions is somewhat equivalent to reducing the pump Rabi frequency since the spectra are determined by the parameters $V_i/\Gamma_{e_ig_i}$.

B. *N* system

In Fig. 5, we compare the absorption spectra for the N system, in the absence and presence of phase-changing collisions. At low intensities, the background absorption widens in the presence of the collisions, and the central feature becomes narrower [see Figs. 5(a) and 5(b)]. As the pump intensity increases, the spectrum in the absence of phase-changing collisions is characterized by four peaks [see Figs. 5(c) and 5(e)] whereas the spectrum in the presence of the collisions has an EIA peak. As in the case of the double TLS system, increasing the rate of collisions is analogous to decreasing the pump intensity. This explains the difference between the spectra in the presence and absence of phase-changing collisions [see Figs. 5(d) and 5(f)]. It should be noted that the spectrum shown in Fig. 5(f) resembles that of Fig. 4(d) of the double TLS in that both consist of a narrow EIA peak inside a wider dip.

Figure 6 shows absorption spectra calculated in the absence of TOC. TOC can be neglected when the excited states are far apart in energy [22]. We see from Figs. 6(a), 6(c), and 6(e), that EIA is absent at all intensities [11]. The addition of phase-changing collisions [see Figs. 6(b), 6(d), and 6(f)] results in spectra that resemble those of the simple TLS, in the presence of phase-changing collisions [21].

VI. DOPPLER BROADENING

We calculate the Doppler broadened probe absorption which is given by

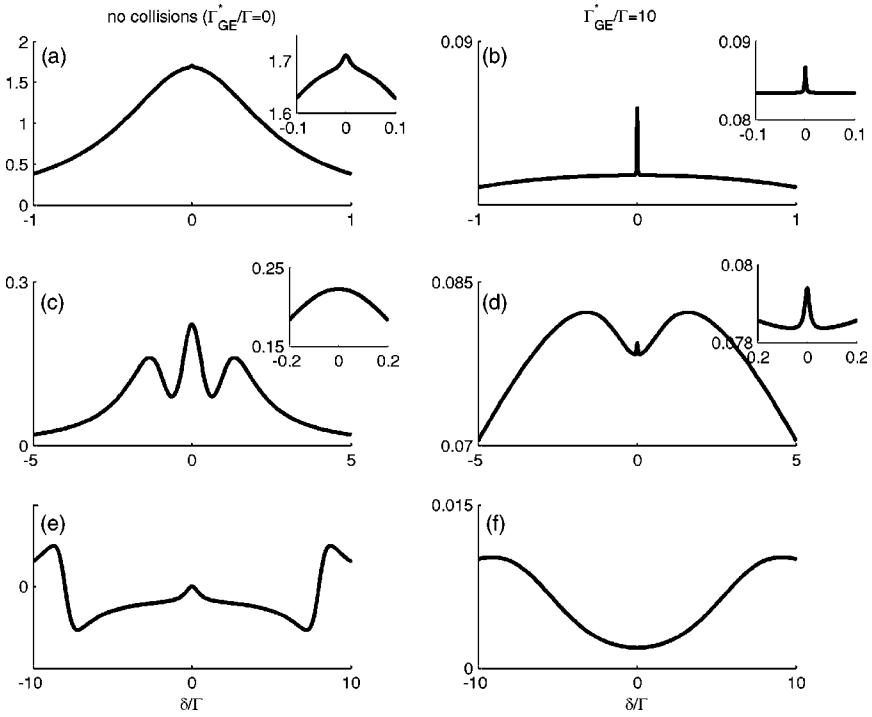

FIG. 4. Calculated probe absorption spectra for the double TLS without (left column), $\Gamma^*_{GE}/\Gamma=0$, and with phase changing collisions (right column), $\Gamma^*_{GE}/\Gamma=10$. In (a) and (b), $V_2/\Gamma=0.1$, in (c) and (d), $V_2/\Gamma=0.5$, and in (e) and (f), $V_2/\Gamma=4$. For all spectra $V_1=0.816V_2$ and $\gamma/\Gamma=0.001$.

$$\alpha(\omega_p)^D = (1/\pi D^2)^{1/2}\int_{-\infty}^{\infty}\alpha(\Delta',\Delta'_p)\exp[-(\Delta-\Delta')^2/D^2]d\Delta', \tag{20}$$

where $\Delta_{1,p}=\omega_{e_i g_i}-\omega_{1,p}$, $\Delta'_p-\Delta_p\simeq\Delta'_1-\Delta_1$, and $D=(2k_BT/m)^{1/2}\omega_0/c$ is the Doppler width.

In Fig. 7, we compare the absorption spectra of the double TLS system, in the absence and presence of Doppler broadening. At low intensity [Figs. 7(a) and 7(b)], the EIA peak is narrowed on Doppler broadening [11]. At higher intensity [Figs. 7(c) and 7(d)], the EIA peak disappears in the absence of Doppler broadening but is found in the presence of Doppler broadening. Its appearance there is due to the interference of the contributions to the Doppler broadened spectrum

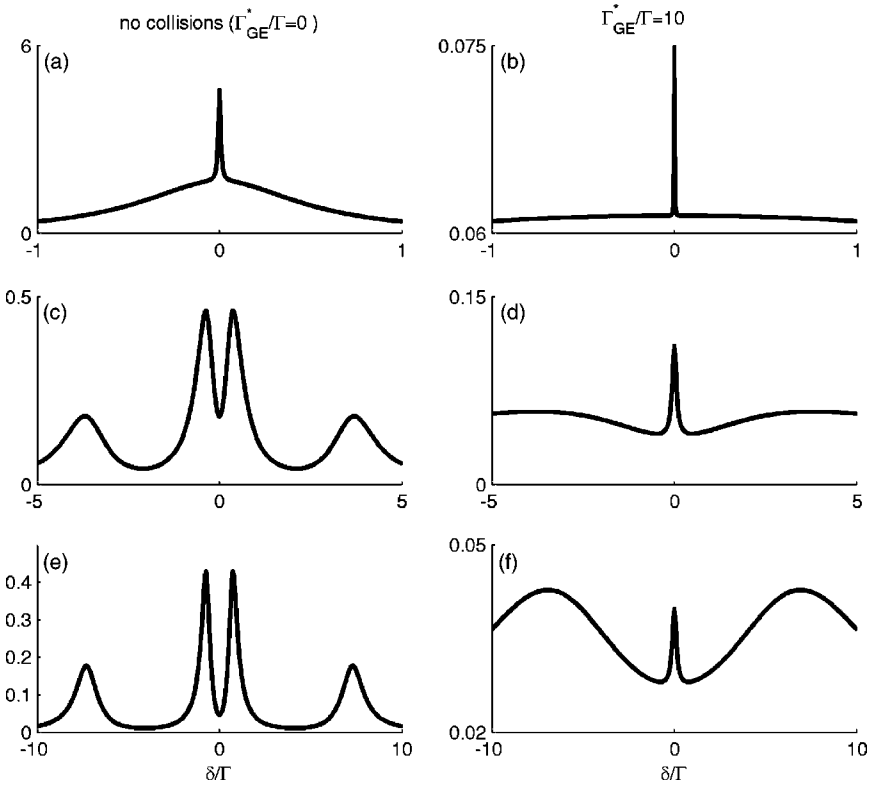

FIG. 5. Calculated probe absorption spectra for the *N* system, which includes TOC, without (left column), $\Gamma^*_{GE}/\Gamma=0$, and with phase changing collisions (right column), $\Gamma^*_{GE}/\Gamma=10$. In (a) and (b), $V_2/\Gamma=0.1$, in (c) and (d), $V_2/\Gamma=2$, and in (e) and (f), $V_2/\Gamma=4$. For all graphs $V_1=0.816V_2$ and $\gamma/\Gamma=0.001$.

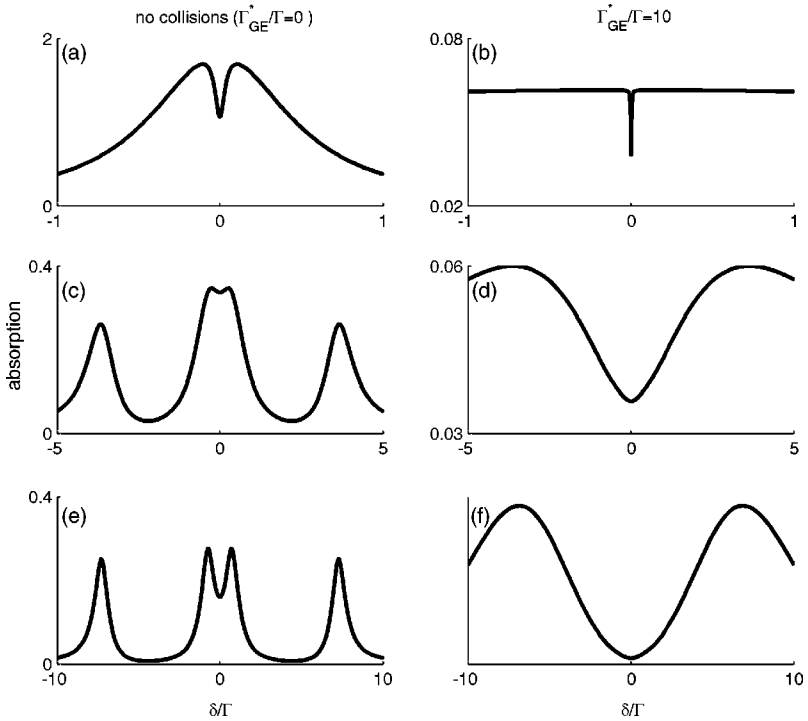

FIG. 6. Calculated probe absorption spectra for the *N* system, in the absence of TOC, without (left column), $\Gamma^*_{GE}/\Gamma=0$, and with phase changing collisions (right column), $\Gamma^*_{GE}/\Gamma=10$. In (a) and (b), $V_2/\Gamma=0.1$, in (c) and (d), $V_2/\Gamma=2$, and in (e) and (f), $V_2/\Gamma=4$. For all graphs $V_1=0.816V_2$ and $\gamma/\Gamma=0.001$.

from $\pm\Delta'$. At even higher Rabi frequencies, the spectra resemble those of the simple TLS, namely, a Mollow spectrum in the absence of Doppler broadening, and a dead zone in the presence of Doppler broadening [14,15].

When phase-changing collisions are introduced, the spectrum (see Fig. 8) resembles the equivalent non-Doppler broadened spectrum [Fig. 4(d)], except that the dip is broader, but still far narrower than the Doppler width, while the central peak is narrowed. This Doppler narrowing has also been noted in the case of EIA-TOC [4,11]. However, there, a dip develops within the peak, whereas, in the case of EIA-TOP, no such dip occurs.

Doppler broadening of the *N* system has been discussed in previous papers [4,11]. The main conclusion was that at low intensity, in the presence of TOC [4], the EIA peak develops a dip. For high pump intensities where the spectrum is characterized by four peaks, Doppler broadening deepens the dip [11].

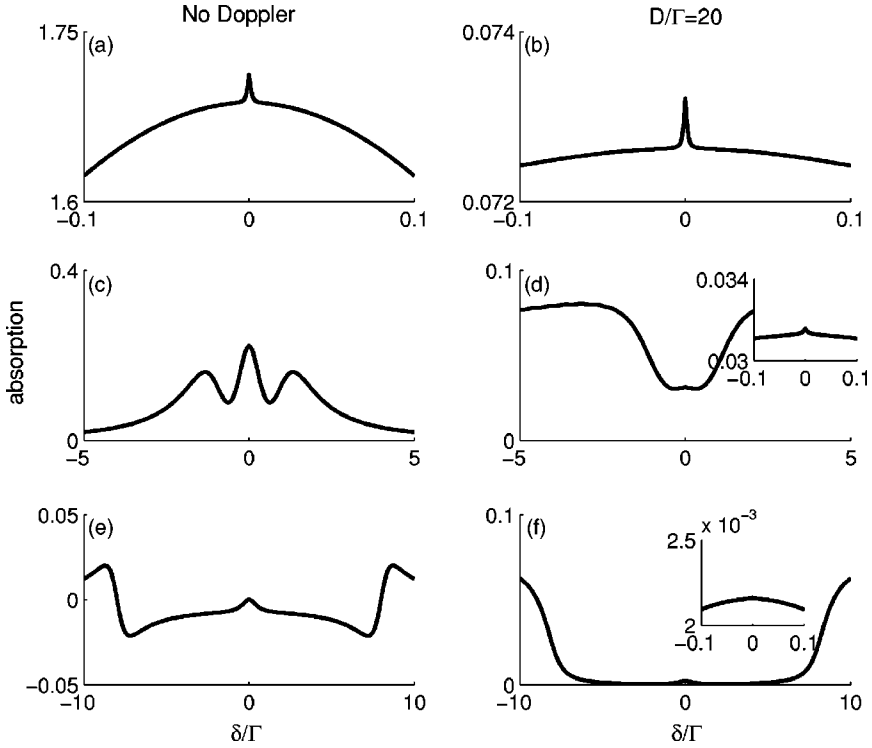

FIG. 7. Calculated probe absorption spectra for the double TLS, without (left column), and with (right column) Doppler broadening ($D/\Gamma=20$). In (a) and (b), $V_2/\Gamma=0.01$, in (c) and (d), $V_2/\Gamma=0.5$, and in (e) and (f), $V_2/\Gamma=4$. For all graphs $V_1=0.816V_2$ and $\gamma/\Gamma=0.001$.

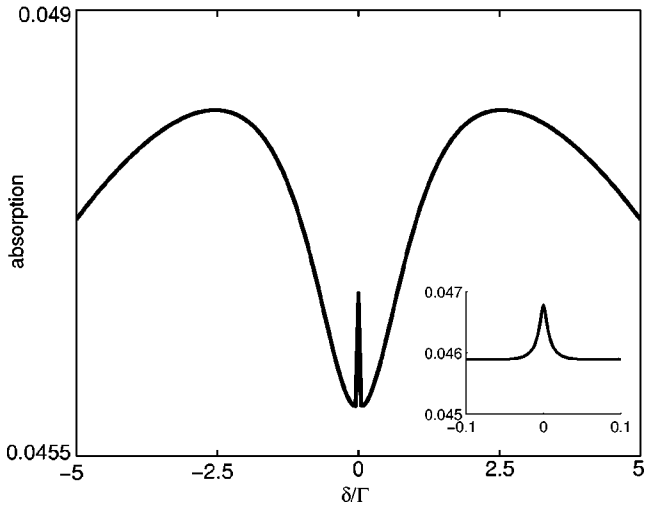

FIG. 8. Collision broadening of Fig. 7(d). $D/\Gamma=20$, $\Gamma^*_{GE}/\Gamma=10$, $V_2/\Gamma=0.5$, $V_1=0.816V_2$ and $\gamma/\Gamma=0.001$. Compare with spectrum of Fig. 4(d), in the absence of Doppler broadening.

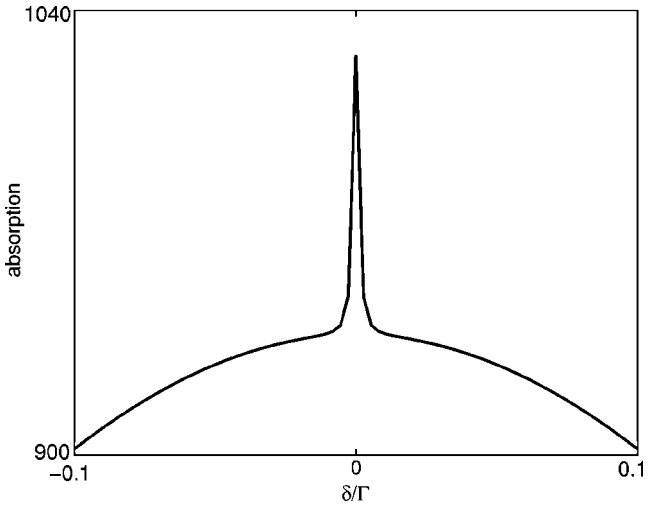

FIG. 10. Realistic atomic system: probe absorption for the cycling $F_g=2\rightarrow F_e=3$ transition of the D_2 line in ^{87}Rb, interacting with a σ_+ polarized resonant pump laser and a tunable σ_+ polarized probe laser, with $\Omega/\Gamma=0.1$. The atomic density was taken to be 10^{12} atoms/cm^3 and $\gamma/\Gamma=0.001$.

We now compare the Doppler-broadened spectra of the N system, in the absence and presence of phase-changing collisions. We see that at low intensity, the peak becomes dramatically narrower on introducing phase-changing collisions [see Figs. 9(a) and 9(b)], as in the case without Doppler broadening [see Figs. 5(a) and 5(b)]. At high intensity, the dip that occurs in the Doppler-broadened spectrum [Fig. 9(c)] becomes less deep when phase-changing collisions are introduced, and can even be totally wiped out by further increasing the rate of phase-changing collisions.

VII. REALISTIC SYSTEMS PUMPED WITH PUMP AND PROBE LASERS WITH THE SAME POLARIZATION

At the pump intensities where EIA-TOP occurs, the double two-level model is not exactly equivalent to any realistic alkali-metal atomic transition. The transitions which most closely correspond to the model are cycling transitions where $F_e=F_g+1$ and $F_g>0$, pumped and probed by σ_+ polarized lasers. In these systems, only the extreme transition $|F_g,m_g=F_g\rangle\rightarrow|F_e,m_e=F_e\rangle$ contributes a peak to the spectrum at line center, whereas the others contribute small dips. The contribution from the extreme transition dominates those from the other transitions for two reasons. First, its ground state has the greatest population since population cannot be pumped out of it, and second, it has the largest transition dipole moment. In Fig. 10 we show the probe absorption spectrum for the $F_g=2\rightarrow F_e=3$ D_2 transition of ^{87}Rb. As the pump intensity increases, the peak shown in Fig. 10 disap-

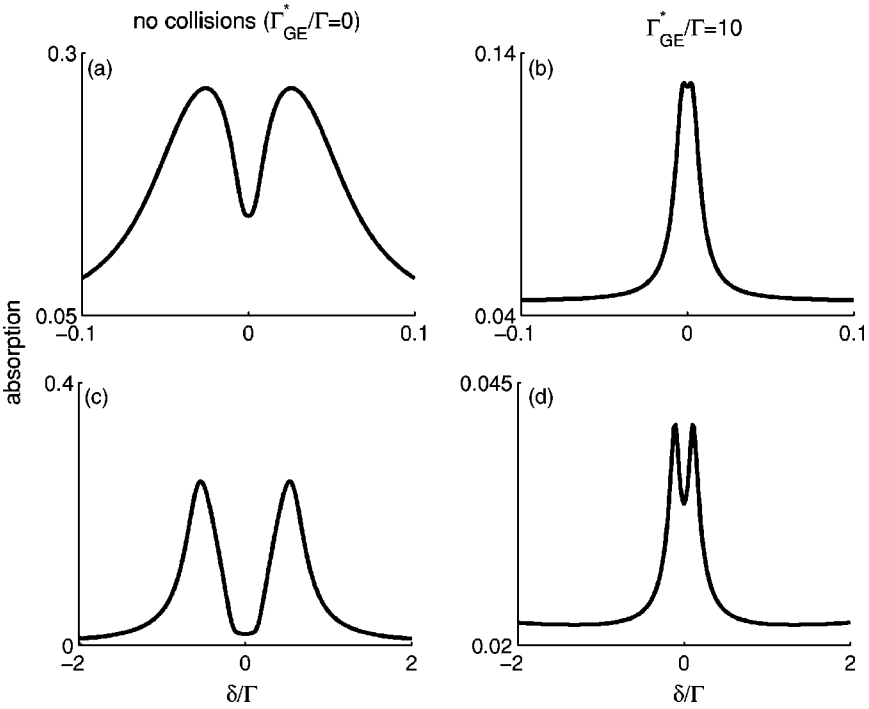

FIG. 9. Doppler broadening, $D/\Gamma=20$, of the N system in the absence (left column) and presence (right column) of phase changing collisions, $\Gamma^*_{GE}/\Gamma=10$. In (a) and (b), $V_2/\Gamma=0.5$, and in (c) and (d), $V_2/\Gamma=4$. For all graphs $V_1=0.816V_2$ and $\gamma/\Gamma=0.001$.

pears, since the population is swept into the extreme state so that the system corresponds to a single TLS. The phenomenon can be observed at higher pump intensities using a transition characterized by higher values of F, such as the $|F_g=4,m_g=4\rangle \rightarrow |F_e=5,m_e=5\rangle$ D_2 transition of ^{133}Cs. Here the pump intensity has to be divided among a larger number of sublevels thus each transition effectively sees a lower intensity. Lipsich *et al.* [23] did not obtain EIA for lasers with parallel polarizations, interacting with an artificially closed $F_g=1$ to $F_e=2$ transition, since the pump intensity used was too high.

EIA-TOP also occurs in realistic cycling transitions pumped and probed with linearly polarized pump and probe lasers. In general the effect is smaller than in the case of σ_+ polarized lasers. The peaks come from those transitions with higher $|m_g|$, whereas the dip are from the transitions with lower $|m_g|$. We discussed the absorption for realistic systems pumped and probed by lasers with different polarizations in Ref. [11].

VIII. CONCLUSIONS

In this paper we show that EIA-TOP can even be obtained for a degenerate TLS where $F_e=F_g+1$ and $F_g>0$, probed by lasers of the same polarization, in the absence of inelastic collisions. We model this EIA-TOP, using a double TLS, pumped and probed by lasers of the same polarization. We compare the probe absorption spectra for the double TLS with those obtained for the N system [11], which is a model for EIA-TOC [3,4]. At low intensity, both model systems give an EIA peak at line center, whereas at high intensity, the double TLS has the same spectrum as a simple TLS and the N system has a spectrum with four peaks. When phase-changing collisions are introduced, the EIA peak is narrowed for both models, and is obtained at higher pump intensities than in the absence of buffer gas. At these intensities, which are different in each model, the central EIA peak is surrounded by a wider dip.

When the double TLS is Doppler broadened in the absence of phase-changing collisions, the spectrum is characterized by EIA at low pump intensities. On increasing the intensity, the spectrum resembles that of a simple TLS, namely a dead zone but with the addition of a small EIA peak at line center which does not exist in the absence of Doppler broadening. When phase-changing collisions are included, the spectra for both models resemble those obtained in the absence of Doppler broadening, namely, a central EIA peak surrounded by a wider dip. In both models, Doppler broadening increases the width of the dip which still remains sub-Doppler. However, the central EIA peak behaves differently in each case: in the double TLS case, the peak becomes narrower on Doppler broadening but, in contrast to the N system, does not develop a dip at line center. In addition, we show here that the dip that appears in the probe absorption spectrum of the N system in the presence of Doppler broadening, can be wiped out by introducing phase-changing collisions. We calculate the EIA-TOP for realistic atomic transitions and show that both σ_+ and linearly polarized lasers give EIA-TOP without inelastic collisions.

[1] A. M. Akulshin, S. Barreiro, and A. Lezama, Phys. Rev. A **57**, 2996 (1998).
[2] A. Lezama, S. Barreiro, and A. M. Akulshin, Phys. Rev. A **59**, 4732 (1999).
[3] A. V. Taichenachev, A. M. Tumaikin, and V. I. Yudin, Phys. Rev. A **61**, 011802(R) (1999).
[4] A. V. Taichenachev, A. M. Tumaikin, and V. Yudin, JETP Lett. **69**, 819 (1999).
[5] C. Goren, A. D. Wilson-Gordon, M. Rosenbluh, and H. Friedmann, Phys. Rev. A **67**, 033807 (2003).
[6] Y. Dancheva, G. Alzetta, S. Cartaleva, M. Taslakov, and C. Andreeva, Opt. Commun. **178**, 103 (2000).
[7] S. K. Kim, H. S. Moon, K. Kim, and J. B. Kim, Phys. Rev. A **68**, 063813 (2003).
[8] A. D. Wilson-Gordon and H. Friedmann, Opt. Lett. **14**, 390 (1989).
[9] C. Affolderbach, S. Knappe, R. Wynands, A. V. Taichenachev, and V. I. Yudin, Phys. Rev. A **65**, 043810 (2002).
[10] C. Goren, A. D. Wilson-Gordon, M. Rosenbluh, and H. Friedmann, Phys. Rev. A **69**, 063802 (2004).
[11] C. Goren, A. D. Wilson-Gordon, M. Rosenbluh, and H. Friedmann, Phys. Rev. A **69**, 053818 (2004).
[12] E. E. Mikhailov, V. A. Sautenkov, Y. V. Rostovtsev, and G. R. Welch, J. Opt. Soc. Am. B **21**, 425 (2004).
[13] E. E. Mikhailov, I. Novikova, Y. V. Rostovtsev, and G. R. Welch, Phys. Rev. A **70**, 033806 (2004).
[14] H. Friedmann and A. D. Wilson-Gordon, Phys. Rev. A **52**, 4070 (1995).
[15] A. Rosenhouse-Dantsker, A. D. Wilson-Gordon, and H. Friedmann, Phys. Rev. A **52**, 4839 (1995).
[16] A. Corney, *Atomic and Laser Spectroscopy* (Oxford University Press, New York, 1986).
[17] E. Alipieva, S. Gateva, E. Taskova, and S. Cartaleva, Opt. Lett. **28**, 1817 (2003).
[18] A. D. Wilson-Gordon and H. Friedmann, Opt. Lett. **8**, 617 (1983).
[19] R. W. Boyd and D. J. Gauthier, *Progress in Optics* (Elsevier, Amsterdam, 2002), Vol. 42.
[20] R. W. Boyd, *Nonlinear Optics*, 2nd ed. (Academic, San Diego, 2003).
[21] R. W. Boyd, M. G. Raymer, P. Narum, and D. J. Harter, Phys. Rev. A **24**, 411 (1981).
[22] P. Dong, A. K. Popov, S. H. Tang, and J.-Y. Gao, Opt. Commun. **188**, 99 (2001).
[23] A. Lipsich, S. Barreiro, A. M. Akulshin, and A. Lezama, Phys. Rev. A **61**, 053803 (2000).